Review of Studies on Corrosion of Steel by CO_2, Focussed on the Behaviour of API Steel in Geological CO_2 Storage Environment

Pregled korozije jekla s CO_2, osredotočen na obnašanja jekel API v okolju geološkega shranjevanja CO_2

Wilmer Emilio García Moreno[1,*], Gabriela Gonçalves Dias Ponzi[1], Ângelo Abel Machado Pereira Henrique[1], Jairo José de Oliveira Andrade[2]

[1] Graduation Programme in Materials Engineering and Technology, Pontifical Catholic University of Rio Grande do Sul (PGTEMA/PUCRS), Brazil

[2] Pontifical Catholic University of Rio Grande do Sul (PGTEMA/PUCRS), Brazil

* wilgm93@gmail.com

Abstract

The world energy demand has become higher with the growing population, which has translated into an increase in emission of greenhouse gases into the atmosphere. For this reason, CO_2 capture and storage has been undertaken to purify the atmosphere. For storing this CO_2, it is necessary to have wells to inject it (deeper than 800 m); moreover, these wells need to have stability over time, and one of the stability aspects is the protection of steel against corrosion. Considering this aspect, the most common steels (focussed on American Petroleum Institute [API] steels) that can be used in an injector well were studied. The best performance was obtained using a high alloy content of Cr and Ni. Furthermore, the most important parameter analysed when corrosion is studied is the test time, which was modelled to stabilise the corrosion rates. The experiments were undertaken after a general review of different studies that investigated the corrosion of steel when in contact with CO_2 in the vapour phase and under supercritical conditions.

Key words: corrosion rate, API steel, CO_2 phase, Cr–Ni–Mo content

Povzetek

Z naraščanjem števila prebivalcev se povečujejo tudi energetske potrebe, kar se odraža na povečanju emisij toplogrednih plinov v atmosfero. Zaradi tega se z namenom čiščenja ozračja izvaja zajem in skladiščenje CO_2. Za skladiščenje CO_2 so potrebne injekcijske vrtine (globlje od 800 m), ki morajo imeti potrebno časovno stabilnost. Eden od stabilnostnih vidikov je ohranjanje jekla proti korozijskim napadom. Zaradi tega so bile opravljene raziskave najbolj pogostih jekel (osredotočeno na API jekla), ki se jih lahko uporablja v injekcijskih vrtinah. Najboljše rezultate so pokazala jekla z visokim deležem Cr in Ni. Pri raziskavah korozije ima pomembno vlogo čas, zato je bil upoštevan pri modelskih analizah. Članek temelji na splošnem pregledu različnih raziskav, v katerih so se avtorji ukvarjali s korozijo jekla v stiku s CO_2 v pari in v superkritičnih pogojih.

Ključne besede: stopnja korozije, API jeklo, faza CO_2, vsebnost Cr-Ni-Mo

Introduction

The economic growth and increasing population have influenced energy demand, causing the latter's cumulative growth, specifically in terms of the use of fossil fuels as a means to supply this demand. This has had repercussion on the global average greenhouse gas concentrations, having CO_2 as the principal component [1]. The biggest challenge in this context is reduction of CO_2 emissions into the atmosphere, with the alternative use of diverse energy sources, such as natural gas, ethanol, nuclear energy, etc. [1].

To reduce the CO_2 level in the atmosphere, CO_2 capture and storage has been planned and used, this CO_2 being stored, mostly, in depleted oil and gas reservoirs; however, some other places have also been considered, such as saline aquifers and coal seams. Some examples of these projects are RECOPOL (coal seam in Poland), Allison Unit (enhanced coal bed methane in Mexico), Selipner (gas field in Norway), Salah gas (project launched by British Petrochemicals and Statoil in Algeria), Ketzin field (enhanced gas recovery in Germany) and some others [2]. According to the Intergovernmental Panel on Climate Change (IPCC) (2007), to have success in CO_2 storage, capacity, injectivity and confinement are required; therefore, well stability is really important, and due to some leakage, a path could be created through the well. Hence, to guarantee the wellbore integrity, some authors have established a lifetime of 1000 years [4–7]. CO_2 is injected in the supercritical condition (>31 °C and 7.38 MPa and stored deeper than 800 m) [2] and reacts with the steel and cement, bringing about damages. When these wells are not designed for injecting CO_2 [3], cement carbonation, microannulus opening and casing corrosion may possibly occur [4]. The objective of this work is to present a general review of the effect of CO_2 corrosion in different kinds of steels used as casing, aiming to know the best options to guarantee the casing stability.

Mechanism of CO_2 Corrosion

Relation Between Corrosion and Well Integrity

When well stability is talked about, an important topic is corrosion (of either steel or cement). However, in this paper, the focus is on steel corrosion. It is important to mention that every completion in wells requires metallic components (wellhead, Christmas tree, tubing, casing, packer, etc.), which – in most of the cases (not always) – are made of some form of steel that have metallic alloy elements, i.e. chromium [5].

A CO_2 injector well can suffer corrosion in every component, from the wellhead to the downhole completion components and, therefore, to achieve large success in the CO_2 storage project, the wells must bear the highest impact of corrosion [2]; thus, to know how to resist corrosion, it is necessary to know how it attacks.

CO_2 is stable, inert and non-corrosive as a gas; however, when it is in the presence of water (either in the aqueous or vapour CO_2 phase), dissolution occurs, with subsequent hydration, forming H_2CO_3 (carbonic acid), which is the principal agent attacking steels [6]; the principal corrosion products are $FeCO_3$ (iron carbonate) and Fe_3C (iron carbide) [7] but, to understand this mechanism better, analysing how it proceeds step by step is required.

Chemical Reaction of CO_2 and H_2O

Following Table 1, first the CO_2 is hydrated by dissolving in water, forming carbonic acid (H_2CO_3), which is a weak acid because the CO_2 is partly dissociated in water. As carbonic acid is diprotic, it dissociates in two steps, which is considered the main source of acidity. The resulting pH is a function of the CO_2 partial pressure. In the first dissociation of carbonic acid, the bicarbonate is obtained (HCO_3), which, later on, dissociates into carbonate (CO_3) [6, 8].

Chemical Interaction of Fe with Environment

Knowing how CO_2 reacts in the presence of water, we can see that Fe also reacts with its environment (Table 2). Initially, Fe reacts with carbonic acid, yielding ferrous bicarbonate ($Fe(HCO_3)_2$); after this, the precipitation

Table 1: *Reaction of CO_2 and H_2O.*

Reaction name	Reaction
Carbon dioxide hydration	$CO_2 + H_2O \leftrightarrow H_2CO_3$
Carbonic acid dissociation	$H_2CO_3 \leftrightarrow H^+ + HCO_3^-$
Bicarbonate anion dissociation	$HCO_3^- \leftrightarrow H^+ + CO_3^{2-}$

Table 2: *Reaction of Fe with the environment.*

Reaction name	Reaction
Iron–carbonic acid reaction	$Fe + 2H_2CO_3 \rightarrow Fe^{2+} + 2HCO_3^- + H_2$
Iron–bicarbonate reaction	$Fe^{2+} + 2HCO_3^- \rightarrow Fe(HCO_3)_2$
Iron carbonate precipitation	$Fe(HCO_3)_2 \rightarrow FeCO_3 + CO_2 + H_2O$
	$Fe^{2+} + CO_3^{2-} \rightarrow FeCO_3$

of iron carbonate occurs, in two ways. First, when the concentrations of Fe^{2+} and CO_3^{2-} ions reach the maximum solubility limit, they combine forming iron carbonate ($FeCO_3$), with a consequent increase in pH [9]. Second, when the ferrous bicarbonate dissociates, it forms $FeCO_3 + CO_2 + H_2O$; this water could react with the resultant carbon dioxide, yielding, again, carbonic acid and, in this way, it could result in a cycle of corrosion.

The case when CO_2 and water are present has been explained, but, normally, water can have different kinds of ions, such as Cl^-, Na^+, Ca^+, SO_1^{2-}, etc., which can affect the equilibrium of CO_2 and the resulting pH [6]. On the other hand, the presence of $FeCO_3$ could lead to a reduction in the corrosion rate because it is formed on the steel surface [10]. Moreover, this protective film is dependent on low temperatures and high supersaturation of Fe^{2+} and CO_3^{2-}; however, this protective film could grow without having any protective property, but, when it does have the property, it could reduce the corrosion rate between 5 and 100 times [8]. Adversely, even when the iron carbonate is precipitated, if it is not compacted on the surface, it cannot prevent the corrosion [10]. Therefore, some analyses have been performed, showing that at low temperatures, the $FeCO_3$ film gets dissolved continuously and the corrosion rate increases [11]. The precipitation kinetics of FeS is almost two
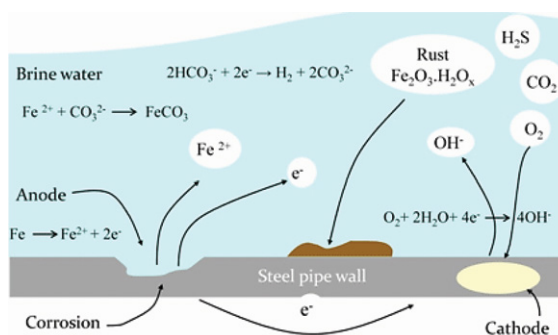
Figure 1: *CO_2 corrosion on a pipe [14].*

orders of magnitude faster than that of $FeCO_3$ at the same conditions [12]; moreover, $FeCO_3$ was formed after 60 days, and even when there was a reduction in corrosion rate, there was still corrosion [13]. In addition, as shown in Figure 1, it is noted that the electrochemical dissociation of iron leads to surface corrosion.

Finally, although the Fe^{2+} ion could react later to form the protective film, this could lead to study the corrosion rate and rate of formation of protective film to know whether $FeCO_3$ is having a positive or negative effect, because as mentioned earlier [11–13], there is still corrosion on steel.
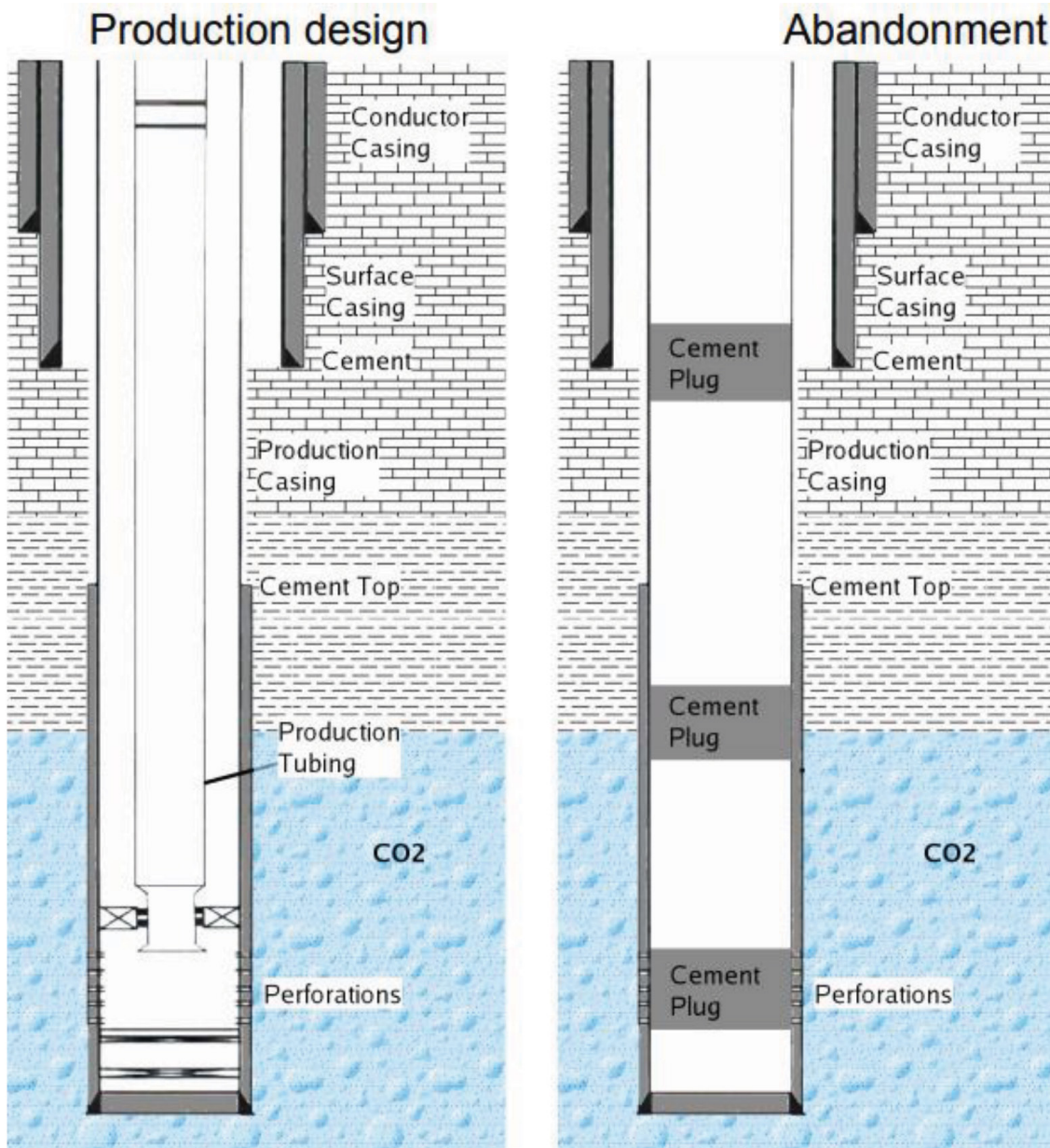
Figure 2: *Well configuration. Taken from [18].*

Different Kinds of Steels

CO_2 can affect the different materials in CO_2 injector wells. Therefore, the metallurgical selection (as well as the type of cement) plays an important role [15] because the casing steel and other parts of the well can be subject to corrosion when they are exposed to CO_2 or formation fluids (or both) (Figure 2). This corrosion can be controlled by using corrosion-resistant alloys (CRAs) [16]. Furthermore, if a CRA is improperly selected, it can lead to mistakes in the future, affecting the performance; hence, taking care of the specific properties of the steels is required because a group of CRAs can be resistant at one temperature; however, this does not guarantee that the CRAs will work with the same performance in a different environment [17].

Casing and tubing play an important role in wells; so, ensuring their integrity is essential. Therefore, the American Petroleum Institute (API) has standardised some grades of steels, which are differentiated by groups, content of

Table 3: *Required chemical composition [21].*

Group	Grade	Type	C Min	C Max	Mn Min	Mn Max	Mo Min	Mo Max	Cr Min	Cr Max	Ni Max	Cu Max	P Max	S Max	Si Max
1	H40	–	–	–	–	–	–	–	–	–	–	–	0.03	0.03	–
	J55	–	–	–	–	–	–	–	–	–	–	–	0.03	0.03	–
	K55	–	–	–	–	–	–	–	–	–	–	–	0.03	0.03	–
	N80	1	–	–	–	–	–	–	–	–	–	–	0.03	0.03	–
	N80	Q	–	–	–	–	–	–	–	–	–	–	0.03	0.03	–
	R95	–	–	0.45	–	1.90	–	–	–	–	–	–	0.03	0.03	0.45
2	M65	–	–	–	–	–	–	–	–	–	–	–	0.03	0.03	–
	L80	1	–	0.43	–	1.90	–	–	–	–	0.25	0.35	0.03	0.03	0.45
	L80	9Cr	–	0.15	0.30	0.60	0.90	1.10	8.00	10.00	0.50	0.25	0.02	0.01	1.00
	L80	13Cr	0.15	0.22	0.25	1.00	–	–	12.00	14.00	0.50	0.25	0.02	0.01	1.00
	C90	1	–	0.35	–	1.20	0.25	0.85	–	1.50	0.99	–	0.02	0.01	–
	T95	1	–	0.35	–	1.20	0.25	0.85	0.40	1.50	0.99	–	0.02	0.01	–
	C110	–	–	0.35	–	1.20	0.25	1.00	0.40	1.50	0.99	–	0.02	0.005	–
3	P110	–	–	–	–	–	–	–	–	–	–	–	0.02	0.03	–
4	Q125	1	–	0.35	–	1.35	–	0.85	–	1.50	0.99	–	0.02	0.01	–

chemical compounds, manufacturing processes and mechanical properties [19], giving the API steel grade; different names are obtained, qualified by a number that represents the minimum yield strength and a letter chosen arbitrarily, without meaning. Therefore, they have been divided into four groups, categorised by resistance to sulphide stress cracking and working pressure [20]:

— Group 1: H-40, J-55, K-55, N-80, R-95;
— Group 2: M-65, L-80, C-90, C-95, T-95, C-110;
— Group 3: P-110;
— Group 4: Q-125.

Furthermore, they can be divided by product specification level (PSL):

— PSL-1: Common application casing (H-40, J-55, K-55, M-65, N-80, R-95);
— PSL-2: Corrosion-resistant casing (L-80, C-90, T-95, C-110);
— PSL-3: Deep well casing (P-110, Q-125).

However, each carbon API steel has the following specific characteristics:

— H40: It is an API steel that is not generally used as tubing, due to its yield strength and

the saving in terms of cost is minimum compared to J55 [19],
— J55: This kind of steel is used for most wells if it meets the design criteria. Moreover, when subjected to a CO_2 environment, it is recommended that it is normalised and tempered, as it is used for maximum 9000 ft and 4000 psi in land wells [19].
— N80: It should be either normalised or normalised and tempered [21]. Furthermore, it shows susceptibility to H_2S, and it is recommended for sweet wells [19].
— L80: Tempered at 620 °C, it has 9Cr and 13Cr steels, being anticorrosive in a CO_2 environment; these types should be used at partial pressure of H_2S <1.5 psi [19],
— T95: It is divided into two types, the first one being used in sour facilities [19].
— C110: This C-steel has maximum minimum yield strength. If necessary, the product can be cold-rotated, straightened and subsequently stress-relieved at temperatures between 30 °C and 55 °C below the final specified tempering temperature, or hot-rotated and straightened at temperatures not >165 °C [21].

Table 4: *Required mechanical properties [22].*

Group	Grade	Type	Elongation (%)	Yield strength (MPa)		Minimum tensile strength (MPa)
				Min	Max	
1	H40	–	0.50	276	552	414
	J55	–	0.50	379	552	517
	K55	–	0.50	379	552	655
	N80	1	0.50	552	758	689
	N80	Q	0.50	552	758	689
	R95	–	0.50	655	758	724
2	M65	–	0.50	448	586	586
	L80	1	0.50	552	655	655
	L80	9Cr	0.50	552	655	655
	L80	13Cr	0.50	552	655	655
	C90	1	0.50	621	724	689
	T95	1	0.50	655	758	724
	C110	–	0.70	758	828	793
3	P110	–	0.60	758	965	862
4	Q125	1	0.65	862	1034	931

— P110: This type is restricted to quench-and-tempered heat treatment and is used in deep and sweet wells with high pressures. Even though it has more yielding strength, it is cheaper than C90 and T95 [19].

— Q125: Gag-press straightening or hot-rotating straightening can be performed for straightening, but the temperature at the end of the rotary straightening process should not be <400 °C. However, if this method cannot be used, the product can also be cold-rotated and straightened, but the stress relief must be performed at 510 °C (950 °F) after straightening [21].

These products must comply with the required chemical composition (Table 3), tensile properties and thickness, as presented in Table 4.

Cr-Steel

Onoyama et al. [23] investigated the corrosion resistance of three different compositions of duplex stainless steel. They evaluated the first two in National Association of Corrosion Engineers (NACE) solution at 80 °C for 100 h to get the effect, in percentage, of different compositions of the alloying elements in the steel, finding that it is desirable to reduce the Si percentage (<0.5%), leading to the amount of Ni becoming 10% and increasing the resistance; moreover, Mo and N improve the steel and, Sn and Sb have to be correctly added, neither in excess or nor in lower amount, with the best values being 0.05% Sn and 0.15% Sb. On the other hand, duplex steel was tested in 2.8×10^{-2} mol/L NaCl solution saturated with CO_2 and N_2 at 260 °C for 100 h at 0.10 and 0.05 MPa, obtaining the maximum value around 8.5×10^{-3} mm/yr at 0.10 MPa of pressure and around 3×10^{-3} mm/yr at 0.05 MPa of pressure.

Kimura et al. [24] studied the effect of CO_2 corrosion in 13Cr steel, modifying the chemical composition of Cu, Ni and Mo, at 3 MPa and 180 °C, inside an autoclave with 20% of NaCl solution saturated with CO_2 gas, for 7 days, evaluating the weight loss rate. When there was no addition of Cu, Ni and Mo, the corrosion rate was 1.71 mm/yr, but when these elements were part of the chemical composition, the corrosion rate was <0.3 mm/yr. Moreover, with the increase in Mo content at the same Ni percentage, the corrosion rate decreased. On the other hand, the addition of Cu did not affect the corrosion rate and- the effect of Ni-Cu was not clear.

Another study was carried out by Leth-Olsen [25], which compared carbon-steel, 13Cr and super 13Cr (S13Cr) in a potassium solution with $CO_{2(g)}$ in the liquid and vapour phases, finding an excellent performance of S13Cr, with an average of 0.01 mm/yr, compared to 13Cr, which had a maximum value of 0.7 mm/yr and 0.3 mm/yr (in the liquid phase). Furthermore, the values of maximum corrosion were noted when the dummies were exposed in the liquid phase, the rates of corrosion in the vapour phase being 0.2 mm/yr for carbon-steel and 0.05 mm/yr for 13Cr; no corrosion was seen in S13Cr.

In 2008, the erosion-corrosion of 22Cr steel was analysed, compared with that of an X65 pipeline under the same conditions. This experiment was evaluated using sand grains under three special conditions. First, by varying the temperature from 20 to 70 °C at a sand concentration of 200 ppm and a CO_2 flow of 20 m/s, a constant corrosion rate of around 5 mm/yr was obtained for 22Cr, while X65 showed an increase from 12.25 to 43.5 mm/yr. Second, the solid particle concentration was varied from 30 to 200 ppm, with a temperature of 20 °C and flow velocity of 20 m/s; although having the same tendency, the corrosion rate for 22Cr increased from 0.1 to 2.4 mm/yr approximately, while for X65, it changed from 9 to 12 mm/yr. The last was the variation of velocity from 7 to 20 m/s, maintaining the temperature at 20 °C and concentration of sand particles at 100 ppm; the corrosion rate in 22Cr increased from 0.2 to 0.8 mm/yr, while for X65, it varied from 2.4 to 5.9 mm/yr approximately [26]. Then, it is important to note that an important parameter is considered in this study, namely, the solid particles.

Xu et al. [7] simulated the 3Cr steel used in the well casing in the Huizhou oilfield, with the same formation water composition to get the effect of CO_2 corrosion at different temperatures (45, 65, 85 and 105 °C), measuring every structure in a CO_2 environment, comparing the result in terms of temperature and CO_2 partial pressure (0.5 and 0.2 MPa). They concluded that by increasing the temperature and pressure, it is possible to gain higher corrosion rates. They observed a corrosion rate of 4.5 mm/yr at CO_2 partial pressure of 0.5 MPa and 100 °C; the

highest value obtained at CO_2 partial pressure of 0.2 MPa was 1.14 mm/yr at 65 °C and approximately 1 mm/yr at 105 °C.

Group 1 (J-55, K-55, N-80)

Cui et al. [27] evaluated the CO_2 corrosion at supercritical conditions (80 °C and 8.274 MPa) in J55, N80 and P110, at different water cuts (30, 50, 70, 90 and 100%), obtaining an increase in corrosion rate with higher water cut amount. Furthermore, N80 and J55 showed similar behaviour (7 and 4 mm/yr) and, at the same time, were better than P110 (9 mm/yr).

Furthermore, Lin et al. [28] compared the three steels mentioned herein at ion concentrations (g/l) of 19.0 Cl^-, 1.14 SO_4^{2-}, 0.6 HCO_3^-, 1.05 Mg_2^+, 0.39 Ca_2^+, 11.99 Na^+ and 0.12 CO_3^2. First, the pressures (6.89 and 10.34 MPa) were varied at 90 °C; the following values were obtained for the corrosion rate of N80, P110 and J55 steels: 1.752 mm/yr, 2.403 mm/yr, 1.854 mm/yr, 0.922 mm/yr, 1.054 mm/yr and 1.105 mm/yr, respectively. Furthermore, when the pressure was maintained constant (between 1.38 and 2.07 MPa CO_2 partial pressure), the corrosion peak was at 100 °C and, after that, it was lower, the best steels being N80 followed by J55.

Some studies have been carried out to compare J-55 and N-80. One on these studies was by Li et al. [29], who analysed the effect of temperature at 5 MPa of partial pressure and varied the partial pressure at 80 °C over a period of 72 h. Furthermore, these two kinds of steel were compared with carbon steel P110: when pressure is varied, the best result was obtained using J55; however, on varying the temperature, sometimes, the best result was obtained using N80.

When this group of steels is talked about, another important steel item referred to is K55. A study was carried out by Elramady [30], in which a piece was subjected in formation water with CO_2 at 40 psi (0.276 MPa) at ambient temperature, obtaining a rate varying from 0.4 to 0.74 mm/yr. On the other hand, Pehlke [31] used brine, CO_2, H_2S and N at 1000 kPa and 170 °C, obtaining a corrosion rate between 0.188 and 0.243 mm/yr for K55 steel.

Furthermore, when corrosion by CO_2 is studied, there are other acids that can affect the well apart from the carbonic acid. Jingen et al. [32]

analysed the effect of the ratio of CO_2 partial pressure to H_2S partial pressure (10, 100, 200 and 400 MPa) in formation water, for N80 steel, at 90 °C and pCO_2 equal to 0.4 MPa, having a flow rate of 1.7 m/s; they found that when H_2S is not present, the corrosion rate is 1.689 mm/yr, while the ratio is 10; the rate is 0.172 mm/yr, changing to 0.789, 0.621 and 0.511 mm/yr for the subsequent ratios. Additionally, another work studied N80 steel at the same temperature, but at 4 MPa in the present of acetic acid with CO_2 in brine. A value of 0.55 mm/yr was obtained in the absence of the acid, but when solid particle concentration was increased to 1000, 3000 and 5000 ppm, the corrosion rate was 1.25, 3.55 and 4.95 mm/yr approximately [33].

Group 2 (L-80, T-95, C-110)

In this group, one of the most commonly used steels is L80. One of the studies on L80 was by Choi et al. [34], where the temperature was set at 65 and 90 °C and the CO_2 pressures used were 4 MPa (gaseous phase) and 8 and 12 MPa (supercritical phase), in a saline solution of 25% HCl; at 65 °C, the corrosion rate

was 8.7, 9.9 and 11 mm/yr, respectively, while at 90 °C, the corrosion rate was 6.1, 3.4 and 4.8 mm/yr, respectively. A similar study was done by Lopes et al. [35], which analysed the steel at 15 and 30 MPa in brine at 50 °C, obtaining 3.534 mm/yr at 15 MPa after 7 days, but 0.375 mm/yr after 30 days and 2.774 mm/yr at 30 MPa after 7 days.

The corrosion process could be affected by other factors, such as sulphur and water. Qiu et al. [36] studied corrosion at three temperatures – 60, 90 and 150 °C – and 0.1 MPa of H_2S partial pressure and 0.5 MPa of CO_2 partial pressure, varying the sulphur content (2 and 4%) and the water content (30 and 70%); the results are shown in Table 5. When the chromium composition of this steel is varied, the corrosion rate changes too, and an example of this is the work by da Silva [37], which used three different CO_2 partial pressures (0.1, 0.3 and 0.65 MPa) at 20 °C with 2, 3 and 5% of NaCl for 72 h, having 0.82% of Cr in twocoupons of L-80 steel (Table 6).

Two other steels in this group are T95 and C110, which were investigated by Elgaddafi [38], where they varied the H_2S concen-

Table 5: *Corrosion rates [36].*

T (°C)	P_{H2S} (MPa)	P_{CO2} (MPa)	Cl⁻ (g/l)	S (%)	H_2O (%)	Rate (mm/yr)
60	0.1	0.5	0.13	2	30	1.56
90	0.1	0.5	0.13	2	30	1.06
150	0.1	0.5	0.13	2	30	1.39
60	0.1	0.5	0.13	4	30	1.47
90	0.1	0.5	0.13	4	30	0.78
150	0.1	0.5	0.13	4	30	2.08
60	0.1	0.5	0.13	2	60	1.15
90	0.1	0.5	0.13	2	60	0.94
150	0.1	0.5	0.13	2	60	0.98
60	0.1	0.5	0.13	4	60	1.10
90	0.1	0.5	0.13	4	60	0.68
150	0.1	0.5	0.13	4	60	1.00

Table 6: *Corrosion rates [37].*

P (bar)	NaCl (%)	Rate (mm/yr)	
		CQ1	CQ2
	2	0.56	0.49
1.0	3	0.45	0.52
	5	8.89	0.29
	2	1.29	0.71
3.0	3	1.26	0.80
	5	1.13	0.82
	2	1.66	1.11
6.5	3	1.57	0.96
	5	1.61	0.92

tration (0, 10, 50 and 150 ppm) at 38 °C and 41.37 MPa; for T95, the CO_2 corrosion rate was 15, 20, 17 and 17.5 mm/yr, while for C110, the values were 13, 14.5 and 9 mm/yr (there was no test for 150 ppm of H_2S).

Groups 3 and 4 (P-110, Q-125)
The last two groups contain only two steels, which are used for deep well casing. Regarding the studies on P110, the first corresponds to analysis at 100 and 160 °C with a pressure of 4 MPa in a brine solution for 120 h, obtaining a marked contrast in corrosion rate, with values of 6.1843 and 0.8754 mm/yr [39]. Similarly, Guan [40] – at 90 °C and 4 MPa – obtained a corrosion rate around 0.8261 mm/yr; at 110 °C with the same pressure, the rate was 0.2489 mm/yr. On the other hand, if the pressure was varied (0.1, 2, 4 and 6 MPa), maintaining the same temperature (100 °C) for 168 h, the results were 0.64, 0.76, 0.91 and 0.83 mm/yr, respectively [41].

The other steel is Q125. This steel was studied in a CO_2 environment, in a brine solution simulated from the Jinlin Oil Field at 1 MPa and 30 °C and a flow of 1 m/s having a corrosion rate of 1.012 mm/yr [42]. Furthermore, varying the temperature (30, 60, 90 and 120 °C) and keeping the pressure at 2 MPa, using formation water from an oilfield, the values obtained were 0.9, 2.8, 3.6 and 2.4 mm/yr [43]. Giving continuity to the investigation from Elgaddafi [38], increasing the H_2S concentration, the corrosion rates were approximately 3.2, 9.5, 10 and 10 mm/yr.

Analysis of CO_2 Corrosion Studies

In this section, the corrosion rates in different kinds of API steels obtained by different studies are analysed. The principal objective was gathering not only the corrosion rate but also data on the chemical composition of chromium, nickel and molybdenum, pressure, temperature, duration of experiment, the phase of CO_2 and the kind of steel. Every detail was collected and summarised in the Appendix.

Dependency of Corrosion Rates on the Test Time
The different values of corrosion rates indicate that corrosion could be dependent on the test time. Hence, these values were plotted against the days on linear (Figure 3) and semi-log (Figure 4) scales to get better information. There is
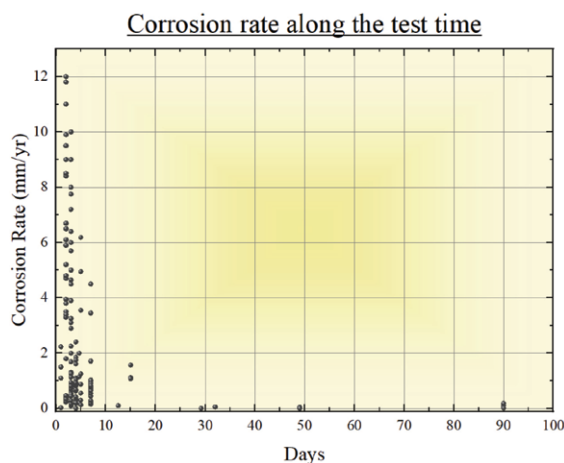
Figure 3: *Corrosion rate against time on a linear scale.*
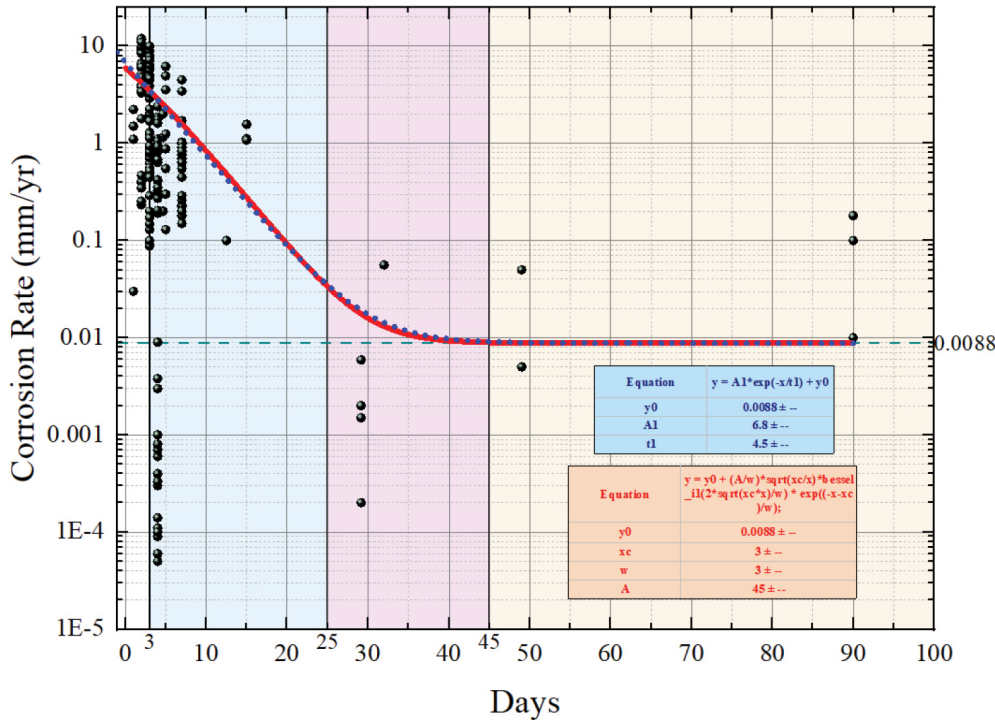
Figure 4: *Corrosion rate against time on a semi-log scale.*

a clear tendency versus the time in the graphs; in Figure 4, four regions were identified:

— From 0 to 3 days, which could be fast growth in corrosion rate, which could be produced by the formation of $FeCO_3$ film.
— From 3 to 25 days, in which there is a continuous reduction of the corrosion rate.
— From 25 to 45 days, stabilisation of the corrosion rates is initiated, with observation of exponentially reducing rates.
— From 45 days onwards, the rates of corrosion are stabilised; there is a plateau, with

a corrosion rate of 0.008 mm/yr; however, this value is only an approximation.

With the already-identified four zones of the corrosion mechanism, the tendency was modelled, yielding two curves; the first equation shows a slightly better fit in the initial region, and the second equation is the best simplified tendency approximation along time (blue dotted curve).

$$y = 0.0088 + \frac{45}{3}\sqrt{\frac{3}{\text{time}}}\left(\frac{2\sqrt{x_0\text{time}}}{3}\right)e^{\frac{-\text{time}-x_0}{3}} \qquad \text{(1): } \textit{Better curve fit}$$

$$y = 0.0088 + 6.8e^{-\frac{\text{time}}{4.5}} \qquad \text{(2): } \textit{The best simplified curve approximation}$$

Stabilised Corrosion Rates

To analyse the long-term corrosion rates, these have to be in their plateau; it means, they have to be stabilised. Therefore, every rate with a test

time below 45 days was stabilised by the mean of the tendency in Eq. (2) (because it is simpler and well fitted). Furthermore, they were separated by the CO_2 phase (vapour and supercrit-

Corrosion rate in CO_2 vapor phase
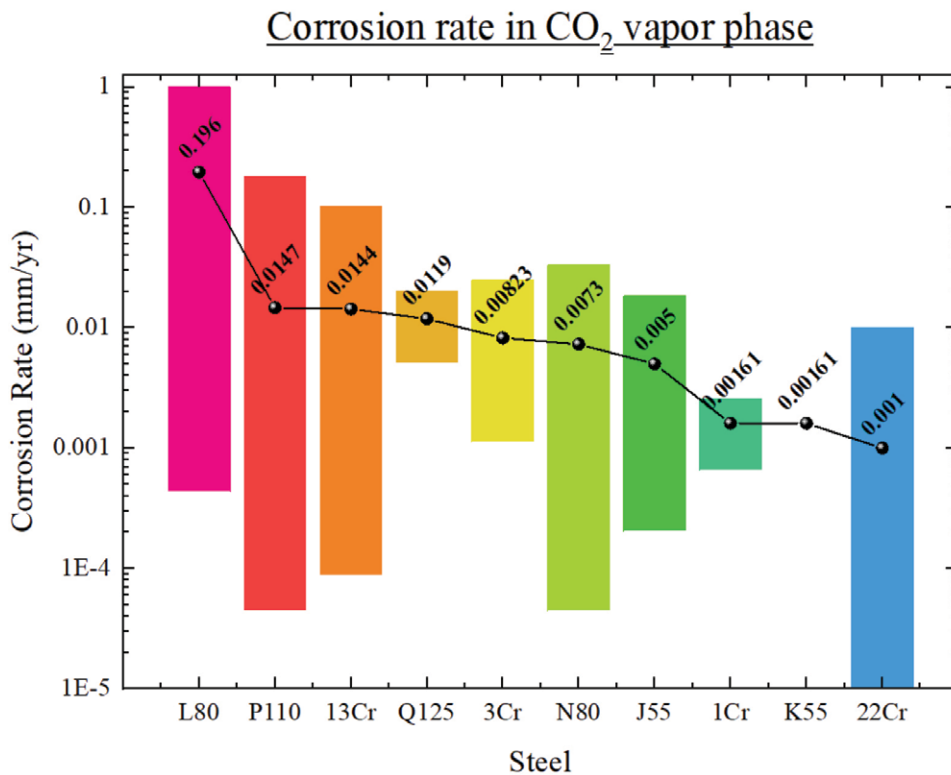
Figure 5: *Stabilised corrosion rates for different kinds of steels in the CO_2 vapour phase.*

Corrosion rate in CO_2 supercritical phase
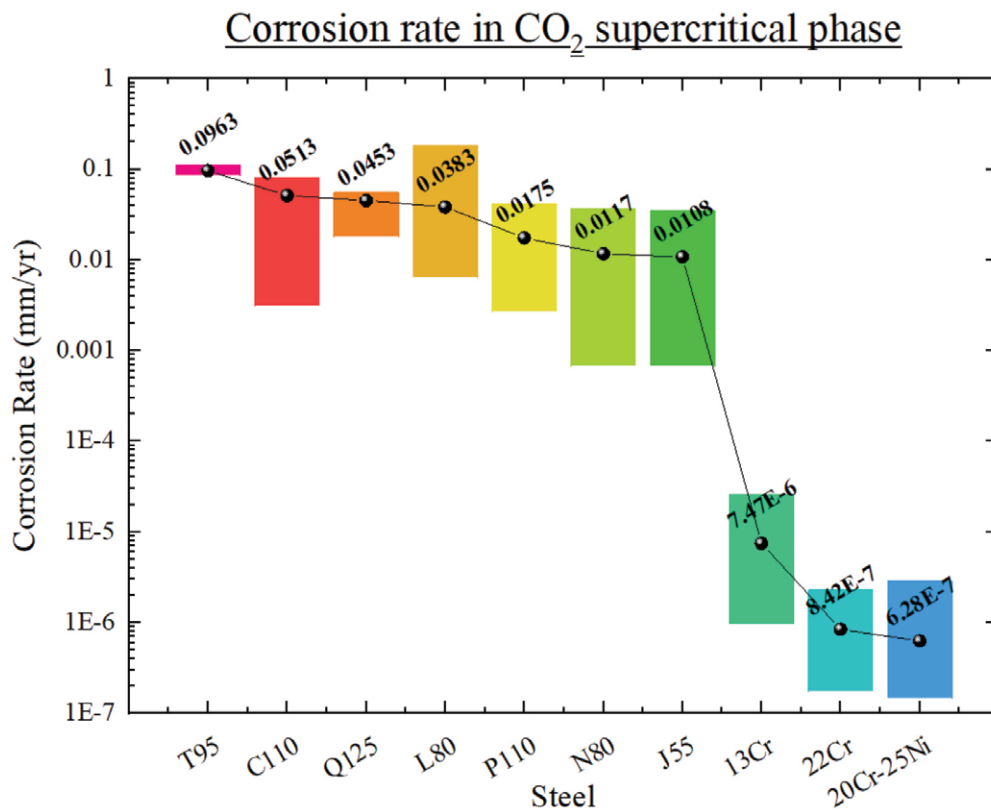
Figure 6: *Stabilised corrosion rates for different kinds of steels in the CO_2 supercritical phase.*

Review of Studies on Corrosion of Steel by CO_2 Focussed on the Behaviour of API Steel in Geological CO_2 Storage Environment

Table 7: *Classification of corrosion rates by steels.*

Category	Steels in CO$_2$ vapour phase	Steels in CO$_2$ supercritical phase
Low	P110, 13Cr, Q125, 3Cr, N80, J55, 1Cr, K55 and 22Cr	P110, N80, J55, 13Cr, 22Cr and 20Cr-25Ni
Moderate	–	T95, C110, Q125 and L80
High	L80	–

Figure 7: *Effect of chromium content in steels, for each CO$_2$ phase.*

ical). Then, to conclude the results observed in both graphs (Figures 5 and 6), it is necessary to refer to the NACE corrosion category, which defines the corrosion rate as low if the value is <0.025 mm/yr, moderate if it ranges between 0.025 and 0.15 mm/yr and high if the value is from 0.16 to 0.25 mm/yr. Thus, the steels could be classified as in Table 7, and in general, the corrosion rate is lower in the supercritical condition, which is the phase of CO$_2$ when it is injected, and higher in the vapour when it goes through the cement paste.

Effect of Chemical Composition of Steels

Addition of chemicals to form steel alloys permit better response against corrosion, especially when chromium is added (it forms stainless steel) and, furthermore, the quantity of nickel and molybdenum could help to prevent CO$_2$ corrosion. The effect of these elements when they are added to steels was analysed (Figures 7–9). There is a clear effect of chromium as a corrosion-protective element. Only its presence in steel reduces corrosion significantly, and at a percentage >20%, it presents a plateau but has a very low corrosion rate. When nickel is added, the rate reduces faster, helping the chro-

Corrosion rate in dependecy of Cr and Ni in each CO$_2$ phase
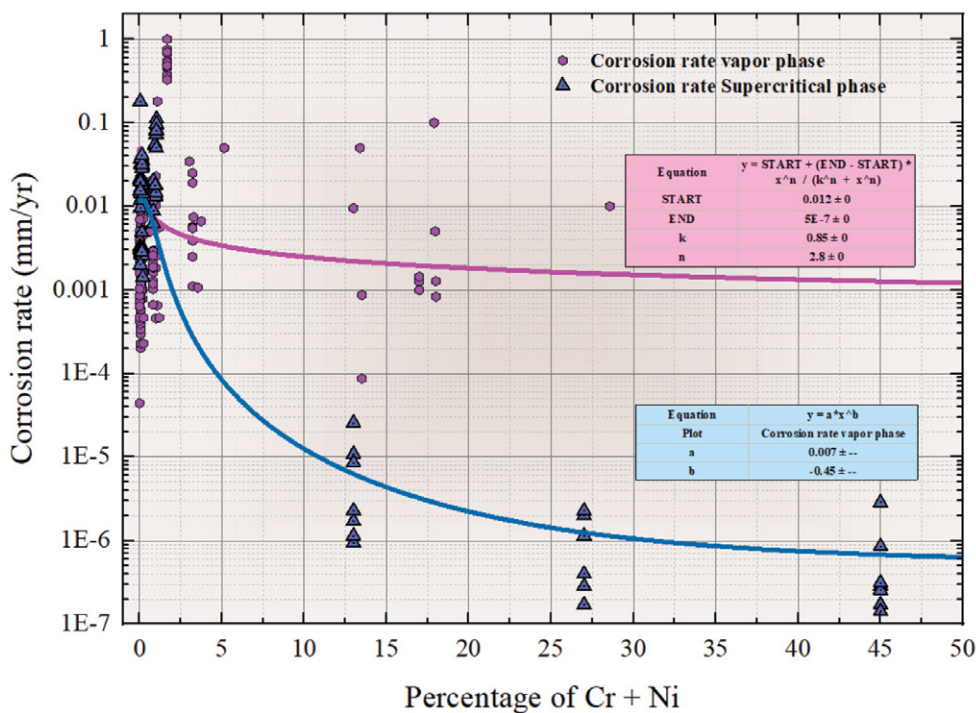
Figure 8: *Effect of chromium and nickel content in steels, for each CO$_2$ phase.*

Corrosion rate in dependency of Cr, Ni and Mo for each CO$_2$ phase

Figure 9: *Effect of chromium, nickel and molybdenum content in steels, for each CO$_2$ phase.*

Corrosion rate vs CO_2 pressure

Figure 10: *Corrosion rate against the pressure.*

Corrosion rate vs temperature for each CO_2 phase

Figure 11: *Corrosion rate versus the temperature.*

mium as a protective element; however, the molybdenum has no significant effect, showing the same tendency as when it is not added. This is in the supercritical condition, because when the vapour phase is observed, the effect is not as high as in the supercritical condition.

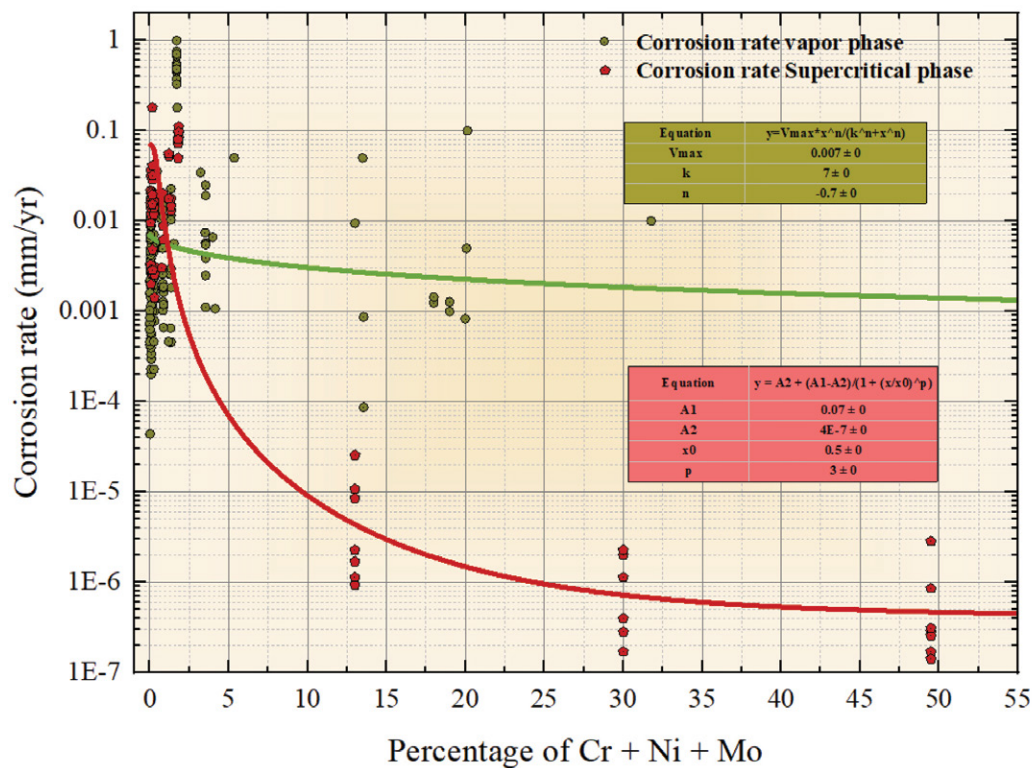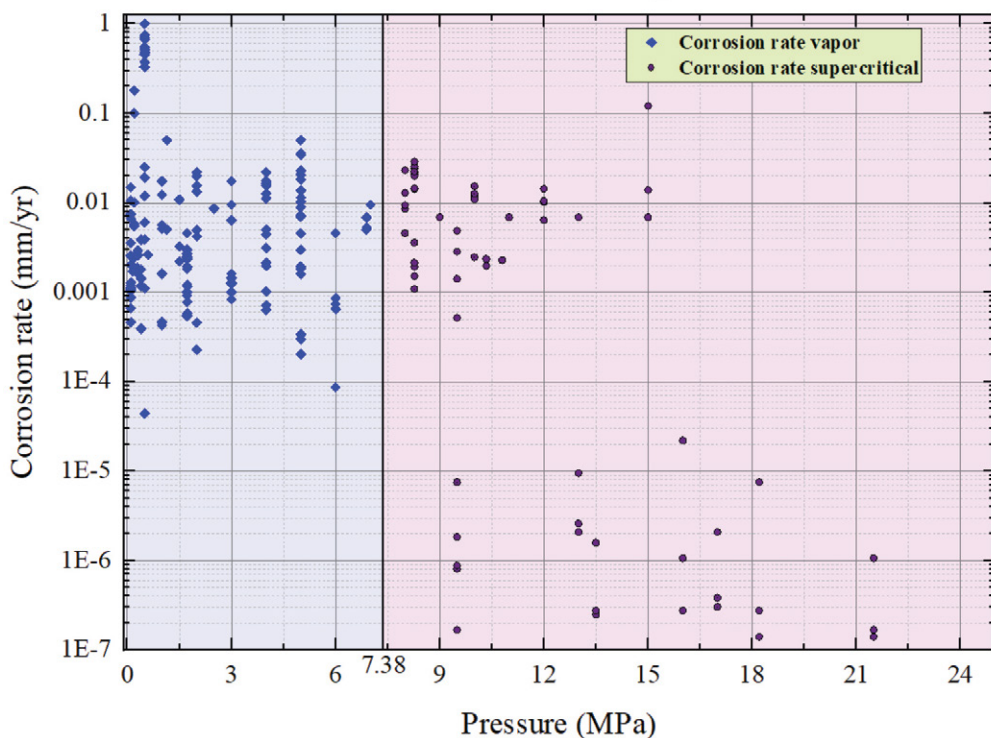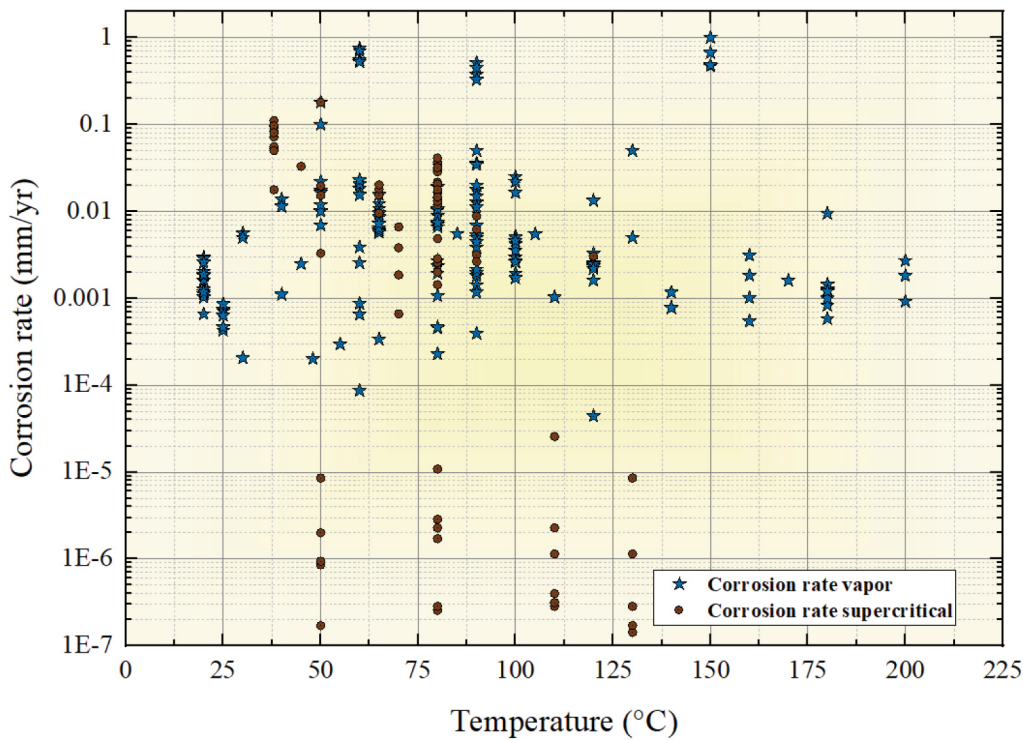### Effect of Pressure and Temperature

Studying the effect of these two factors is difficult, because the idea is to analyse by varying one of them and maintaining the other one constant; to observe the effect, however, it was decided to graphically represent them as separate parameters (Figures 10 and 11). Then, varying the pressure (>7.38 MPa is supercritical condition), the lowest corrosion rates are found in the supercritical conditions, and as the pressure becomes higher, lower rates are obtained. However, when the temperature is evaluated, it is difficult to get a tendency probably because different values of pressure could be studied at one temperature.

Conclusion

It is known that different factors could affect the corrosion rates. First, the time of tests has to be considered because a test spreading over 3 days should not be used for determining awell's stability in CO_2–rich conditions, because, as earlier mentioned, for a warranty of stability for >100 years, the corrosion rates must be the lowest as possible. On the other hand, the wall thickness is a factor to be considered in the front side corrosion rates, because the walls could be as thick as 12 mm to >25 mm. Thus, a corrosion rate of 0.06 mm/yr could corrode half the thickness of a wall of 12 mm in 100 years; hence, warrantying the lowest corrosion rates is extremely important and required.

Alternatively, having a steel with high yield strength, such as C110, T95 or P110, is not a warranty for having good corrosion protection, but the chemical elements can help. Furthermore, ensuring good corrosion protection during the injection of CO_2 can have the highest effect on the life of the casing and tubing along the well, because, besides the corrosion, the steel can be affected by erosion due to the flow of CO_2 along the tubing. Additionally, if the well presents good stability along its injection path, the next important section has to be the cement paste stability, which will be the wall between the casing and the stored CO_2. Furthermore, the only steel that presented a relatively worse behaviour was L80, but in the vapour phase of CO_2. Finally, by ensuring a corrosion rate around 0.01 mm/yr, in 1000 years, it will corrode 10 mm; but for this to happen, the CO_2 has to be in contact with the casing. It means an injectivity spanning 1000 years or breaking through the cement paste after storing.

Acknowledgements

References

[1] M. Zhang and S. Bachu, "Review of integrity of existing wells in relation to CO2 geological storage: What do we know?," *International Journal of Greenhouse Gas Control,* vol. 5, pp. 826–840, 2011.

[2] M. Bai, Z. Zhang and X. Fu, "A review on well integrity issues for CO2 geological storage and enhanced gas recovery," *Renewable and Sustainable Energy Reviews,* vol. 59, pp. 920–926, 2016.

[3] S. Bachu and T.L. Watson, "Review of failures for wells used for CO2 and acid gas injection in Alberta, Canada," *Energy Procedia,* vol. 1, no. 1, 2009.

[4] S. Asamoto, Y.L. Guen, O. Poupard and B. Capra, "Well integrity assessment for CO2 injection – A numerical case study on thermo-mechanical behavior in downhole CO2 environments," *Engineering Computations,* vol. 30, no. 6, pp. 842–853, 2013.

[5] J. Bellarby, "Material Selection," in *Well Completion Design,* vol. 56, Developments in Petroleum Science, 2009, pp. 433–472.

[6] A. Kahyarian, M. Achour and S. Nešić, "CO2 corrosion of mild steel," in *Trends in Oil and Gas Corrosion Research and Technologies*, Woodhead Publishing Series in Energy, 2017, pp. 149–190.

[7] L. Xu, J. Xu, M.-b. Xu, S.-y. Li, S. Liu, Y. Huang and F.-c. You, "Corrosion Behavior of 3% Cr Casing Steel in CO2-Containing Environment: A Case Study," *The Open Petroleum Engineering Journal,* vol. 11, pp. 1–13, 2018.

[8] A. Dugstad, "Fundamental Aspects of CO2 Metal Loss Corrosion – Part I: Mechanism," 2006.

[9] M. Nordsveen, S. Nešić, R. Nyborg and A. Stangeland, "A Mechanistic Model for Carbon Dioxide Corrosion of Mild Steel in the Presence of Protective Iron Carbonate Films—Part 1: Theory and Verification," *Corrosion,* vol. 59, no. 5, pp. 443–456, 2003.

[10] T. Li, Y. Yang, K. Gao and M. Lu, "Mechanism of protective film formation during CO2 corrosion of X65 pipeline steel," *Journal of University of Science and Technology Beijing,* vol. 15, no. 6, 2008.

[11] J. Hernandez, A. Muñoz and J. Genesca, "Formation of iron-carbonate scale-layer and corrosion mechanism of API X70 pipeline steel in carbon dioxide-saturated 3% sodium chloride," *Afinidad IQS,* vol. 69, 2012.

[12] Z. Ma, Y. Yang, B. Brown, S. Nesic and M. Singer, "Investigation of FeCO3 and FeS Precipitation Kinetics by EQCM," in *NACE International 2018*, 2018.

[13] T. Berntsen, M. Seiersten and T. Hemmingsen, "Effect of FeCO3 Supersaturation and Carbide Exposure on the CO2 Corrosion Rate of Carbon Steel," *Corrosion Sciences,* vol. 69, no. 6, 2013.

[14] S. Ibrahim, "isalama," [Online]. Available: https://isalama.wordpress.com/article/corrosion-inhibitors-in-the-oilfield-3uf3kbfllnswt-4/. [Accessed 7 December 2019].

[15] M. Haigh, "Well Design Differentiators for CO2 Sequestration in Depleted Reservoirs," *Society of Petroleum Engineers,* 2009.

[16] T. Syed and T. Cutler, "Well Integrity Technical and Regulatory Considerations for CO2 Injection Wells," *Society of Petroleum Engineers,* 2010.

[17] B.D. Craig and L. Smith, Corrosion Resistant Alloys (CRAs) in the oil and gas industry, Nickel Institute, 2011.

[18] B. Carey, "IEA Greenhouse Gas," [Online]. Available: https://ieaghg.org/docs/General_Docs/Summer_School/CAREY%20Wellbore%20Integrity_Tues_secured.pdf. [Accessed 12 December 2019].

[19] Equip Outlet Inc, "API Steel Grade Category and Color," 2017. [Online]. Available: http://www.equipoutlet.com/api-steel-grade-category.html. [Accessed 28 April 2019].

[20] OEA Consulting, "The API Casing Steel Grades... How Are They Defined?," OEA Consulting, 2018. [Online]. Available: https://www.oea-consulting.ca/our-blog/13-the-api-casing-steel-grades-how-are-they-defined. [Accessed 28 April 2019].

[21] OCTAL Steel, "API 5CT Casing and Tubing Specification," OCTAL Steel, 31 January 2019. [Online]. Available: https://www.octalsteel.com/api-5ct-specification. [Accessed 28 April 2019].

[22] API, "API Specification 5CT 9th Edition," API, 2011.

[23] M. Onoyama, N. Hayashi, K. Shitani and T. Suehiro, "Evaluation of Corrosion Resistance of a Duplex Stainless Steel in H2S-CO2-Chloride Environments," *Material for energy systems,* vol. 5, no. 2, 1983.

[24] M. Kimura, Y. Miyata, Y. Yamane, T. Toyooka, Y. Nakano and F. Murase, "Corrosion Resistance of High-Strength Modified 13% Cr Steel," *Corrosion Science,* 1999.

[25] H. Leth-Olsen, "CO2 Corrosion of Steel in Formate Brines for Well Applications," in *Corrosion 2004*, 2004.

[26] X. Hu and A. Neville, "Erosion-corrosion of Pipeline Steel X65 and 22Cr Duplex Stainless Steel in CO2 Saturated Environment," in *SPE International Oilfield Corrosion Conference*, Aberdeen, 2008.

[27] Z. Cui, S. Wu, C. Li, S. Zhu and X. Yang, "Corrosion behavior of oil tube steels under conditions of multiphase flow saturated with super-critical carbon dioxide," *Materials Letters,* vol. 58, no. 6, pp. 1035–1040, 2004.

[28] G. Lin, M. Zheng, Z. Bai and X. Zhao, "Effect of Temperature and Pressure on the Morphology of Carbon Dioxide Corrosion Scales," *Corrosion Science,* vol. 62, no. 6, June 2006.

[29] N. Li, D. Xu, W. Ma, P. Ma and J. Li, "CO2 Corrosion Behaviors of Tubing and Casing Steels in Simulation Produced Water for Deep Natural Gas Wells," in *5th International Conference on Advanced Engineering Materials and Technology (AEMT 2015)*, 2015.

[30] A.G. Elramady, "The Effect of various deformation processes on the corrosion behavior of casing and tubing carbon steels in sweet environment," 2015.

[31] T. Pehlke, "Studies of Aqueous Hydrogen Sulfide Corrosion in Producing SAGD Wells," University of Calgary, Calgary, 2017.

[32] D. Jingen, Y. Wei, L. Xiaorong and D. Xiaoqin, "Influence of H2S Content on CO2 Corrosion Behaviors of N80 Tubing Steel," *Petroleum Science and Technology,* pp. 1387–1396, 2011.

[33] S. Zh, A. Fu, J. Miao, Z. Yin and J. Wei, "Corrosion of N80 carbon steel in oil field formation water containing CO2 in the absence and presence of acetic acid," *Corrosion Science,* vol. 53, no. 53, pp. 3156–3165, 2011.

[34] Y.-S. Choi, F. Farelas, S. Nešić, A.A.O. Magalhães and C. d. A. Andrade, "Corrosion Behavior of Deep Water Oil Production Tubing Material Under Supercritical CO2 Environment: Part 1—Effect of Pressure and Temperature," *Corrosion Science,* vol. 70, no. 1, pp. 38–47, 2014.

[35] N.F. Lopes, E.M. da Costa and J.S. Fernandes, "Desempenho do aço API L80 frente à corrosão por CO2 em meio similar ao pré-sal," in *22º CBECiMat - Congresso Brasileiro de Engenharia e Ciência dos Materiais*, Natal, 2016.

[36] Z. Qiu, C. Xiong, R. Yi and Z. Ye, "Corrosion Behavior of L80Steel in Different Temperature and Sulfur Content," *IOP Conference Series: Materials Science and Engineering,* 2017.

[37] P. da Silva Neto, "Desenvolvimento de Tubo de Aço API 5CT Grau L80 com 1% Cromo Soldado por ERW/HFIW," UFRJ, Rio de Janeiro, 2016.

[38] R. Elgaddafi, R. Ahmed and S. Shah, "Modeling and experimental studies on CO2-H2S corrosion of API carbon steels under high-pressure," *Journal of Petroleum Science and Engineering,* vol. 156, pp. 682–696, 2017.

[39] Z. Yin, W. Zhao, Z. Bai and Y. Feng, "Characteristics of CO2 corrosion scale formed on P110 steel in simulant solution with saturated CO2," *Surface and Interface Analysis,* vol. 40, no. 9, pp. 1231–1236, 2008.

[40] Z. Guan, Y. Ren, Z. Cui, J. Zhang and M. Du, "Evaluation of Corrosion Inhibitors for P110 Steel in Simulated Oilfield Produced Waters Using EFM and CMAS Techniques," *Corrosion Science and Protetion Technology,* vol. 28, no. 2, pp. 139–143, 2016.

[41] J. Li, H. Ma, S. Zhu, C. Qü and Z. Yin, "Erosion resistance of CO2 corrosion scales formed on API P110 carbon steel," *Corrosion Science,* vol. 86, pp. 101–107, 2014.

[42] L. Wang, F. Liu, Q. Zhao and H.-b. Wu, "CO2 Corrosion and Grooving Corrosion Behavior of the ERW Joint of the Q125 Grade Tube Steel," *Journal of Iron and Steel Research, International,* vol. 22, no. 10, pp. 943–948, 1015.

[43] D. Tang, L. Wang, H. Wu and i. Liang, "Mechanical Properties and CO2 Corrosion Behavior of Q125 Grade Oil Tube Steel Used in Deep Oil Well," *Advanced Materials Research,* Vols. 524–527, pp. 1471–1479, 2012.

[44] Y. Zhang, K. Gao and G. Schmitt, "Water Effect On Steel Under Supercritical CO2 Condition," in *Corrosion Conference 2011*, Texas, 2011.

[45] A. Pfennig and R. Bäßler, "Effect of CO2 on the stability of steels with 1% and 13% Cr in saline water," *Corrosion Science,* vol. 51, pp. 931–940, 2009.

[46] W. Yan, P. Zhu and J. Deng, "Corrosion behaviors of SMSS 13Cr and DSS 22Cr in H2S/CO2-oil-water environment," *International journal of electrochemical science,* vol. 11, no. 11, pp. 9542–9558, 2016.

[47] S. Azuma, H. Kato, Y. Yamashita, K. Miyashiro and S. Saito, "The Long-term Corrosion Behaviour of Abandoned Wells Under CO2 Geological Storage Conditions: (2) Experimental Results for Corrosion of Casing Steel," *Energy Procedia,* vol. 37, pp. 5793–5803, 2013.

[48] H. Bai, Y. Wang, Y. Ma, Q. Zhang and N. Zhang, "Effect of CO2 Partial Pressure on the Corrosion Behavior of J55 Carbon Steel in 30% Crude Oil/Brine Mixture," *Materials,* vol. 11, no. 9, 2018.

[49] X.Z. Wang, Z.G. Yang, Z.F. Yin, Z.Q. Gao, J.D. Li and K. Wang, "Corrosion investigation of J55 steel under simulated enhanced oil recovery conditions using CO2 flooding," *Corrosion Engineering, Science and Technology,* vol. 49, no. 4, pp. 275–282, 2014.

[50] Y. Ma, Q. Zhang and H. Bai, "N80 Oil Tube Steel Corrosion Behavior in Different CO2 Saturated Brine," *Ekoloji,* no. 106, pp. 113–121, 2018.

[51] H. Li, D. Li, L. Zhang, Y. Bai, Y. Wanga and M. Lua, "Fundamental aspects of the corrosion of N80 steel in a formation water system under high CO2 partial pressure at 100 °C," *RSC Advances,* no. 21, 2019.

[52] M. Escalante, N. Ochoa, C. Sequera and J. Jaspe, "Evaluación de la resistencia a la corrosión por CO2 de nuevos aceros de bajo cromo utilizados en tubulares de pozo mediante tecnicas electroquímicas," *Revista Latinoamericana Met. Mat,* vol. 34, no. 1, 2014.

[53] X. Zhang, J.F. Zevenbergen and T. Benedictus, "Corrosion Studies on Casing Steel in CO2 Storage Environments," *Energy Procedia,* vol. 37, pp. 5816–5822, 2013.

[54] M.N. Hazman bin Mansor, *Study on C02 Corrosion in Oil Producing Well,* 2009.

[55] L.C. Lozada, *Corrosion performance of L80, L80Cr1% and L80Cr3% steel grades in simulant solution with carbon dioxide and scaling,* Manchester, 2015.

[56] C. Ren, D. Zeng, J. Lin, T. Shi and W. Chen, "Sour Corrosion of C110 Steel and Its Influence by Galvanic Couple and Stress," *Industrial and Engineering Chemistry Research,* vol. 51, no. 13, p. 4894–4904, 2012.

[57] J. Sun, C. Sun, X. Lin, X. Cheng and H. Liu, "Effect of Chromium on Corrosion Behavior of P110 Steels in

CO2-H2S Environment with High Pressure and High Temperature," *Materials,* vol. 9, no. 3, 2016.

[58] Y.D. Cai, P.C. Guo, D.M. Liu, S.Y. Chen and J.L. Liu, "Comparative study on CO2 corrosion behavior of N80, P110, X52 and 13Cr pipe lines in simulated stratum water," *Science China Technological Sciences,* vol. 53, no. 9, p. 2342–2349, 2010.

[59] R. Xie, Z. Gu, Y. Yao, H. Xu, K. Deng and Y. Liu, "Electrochemical Study on Corrosion Behaviors of P110 Casing Steel in a Carbon Dioxide-Saturated Oilfield Formation Water," *International journal of electrochemical science,* vol. 10, no. 7, pp. 5756–5769, 2015.

[60] IPCC, "Climate Change 2014 Synthesis Report Summary for Policymakers," 2014.

[61] B.G. Kutchko, B.R. Strazisar, D.A. Dzombak, G.V. Lowry and N. Thaulow, "Degradation of Well Cement by CO2 under Geologic Sequestration Conditions," *Environmental and Science Technology,* p. 4787–4792, 7 May 2007.

[62] V. Barlet-Gouédard, G. Rimmelé, O. Porcherie, N. Quisel and J. Desroches, "A solution against well cement degradation under CO2 geological storage environment," *International Journal of Greenhouse Gas Control,* vol. 3, no. 2, pp. 206–216, March 2009.

[63] Y. Kohei, S. Satoko, K. Hiroyasu, M.J. Stenhouse, Z. Wei, P. Alexandros, Y. Yuji, M. Kazutoshi and S. Shigeru, "The Long-term Corrosion Behavior of Abandoned Wells Under CO2 Geological Storage Conditions: (3) Assessment of Long-term (1,000-year) Performance of Abandoned Wells for Geological CO2 Storage," *Energy Procedia,* vol. 13, pp. 5804–5815, 2013.

[64] R. Beckwith, "Carbon Capture and Storage: A Mixed Review," *Journal of Petroleum Technology,* 2011.

Appendix

Steel	CO$_2$ phase	P (MPa)	T (°C)	Rate (mm/yr)	Reference	Time (days)	C	Cr	Ni	Mo
3Cr	Vapour	0.2	45	0.45	[7]	7	0.22	2.94	0.3	0.3
3Cr	Vapour	0.2	65	1.03	[7]	7	0.22	2.94	0.3	0.3
3Cr	Vapour	0.2	85	1	[7]	7	0.22	2.94	0.3	0.3
3Cr	Vapour	0.2	105	0.99	[7]	7	0.22	2.94	0.3	0.3
3Cr	Vapour	0.5	40	0.2	[7]	7	0.22	2.94	0.3	0.3
3Cr	Vapour	0.5	60	0.7	[7]	7	0.22	2.94	0.3	0.3
3Cr	Vapour	0.5	80	3.45	[7]	7	0.22	2.94	0.3	0.3
3Cr	Vapour	0.5	100	4.5	[7]	7	0.22	2.94	0.3	0.3
13Cr	Vapour	3	180	1.71	[24]	7	0.025	13		
13Cr	Vapour	3	180	0.225	[24]	7	0.025	13	4	1
13Cr	Vapour	3	180	0.18	[24]	7	0.025	13	4	2
13Cr	Vapour	3	180	0.23	[24]	7	0.025	13	5	1
13Cr	Vapour	3	180	0.15	[24]	7	0.025	13	5	2
13Cr	Vapour	3	180	0.26	[24]	7	0.025	13	4	1
13Cr	Vapour	3	180	0.18	[24]	7	0.025	13	4	2
13Cr	Vapour	1.14	130	0.05	[25]	49	0.02	13	0.4	0.09
13Cr	Vapour	1.14	130	0.005	[25]	49	0.02	12.24	5.73	2.1
J55	Supercritical	8.274	80	0.5	[27]	4	0.19	0.19	0.017	0.092
J55	Supercritical	8.274	80	0.9	[27]	4	0.19	0.19	0.017	0.092
J55	Supercritical	8.274	80	7	[27]	4	0.19	0.19	0.017	0.092
J55	Supercritical	8.274	80	10.5	[27]	4	0.19	0.19	0.017	0.092
J55	Supercritical	8.274	80	12.2	[27]	4	0.19	0.19	0.017	0.092
N80	Supercritical	8.274	80	0.7	[27]	4	0.24	0.036	0.028	0.021
N80	Supercritical	8.274	80	1	[27]	4	0.24	0.036	0.028	0.021
N80	Supercritical	8.274	80	7.2	[27]	4	0.24	0.036	0.028	0.021
N80	Supercritical	8.274	80	11	[27]	4	0.24	0.036	0.028	0.021
N80	Supercritical	8.274	80	12.8	[27]	4	0.24	0.036	0.028	0.021
P110	Supercritical	8.274	80	1	[27]	4	0.26	0.15	0.012	0.01
P110	Supercritical	8.274	80	1.7	[27]	4	0.26	0.15	0.012	0.01
P110	Supercritical	8.274	80	10	[27]	4	0.26	0.15	0.012	0.01
P110	Supercritical	8.274	80	11.2	[27]	4	0.26	0.15	0.012	0.01
P110	Supercritical	8.274	80	14.4	[27]	4	0.26	0.15	0.012	0.01
J55	Vapour	6.89	90	1.854	[28]	4	0.19	0.19	0.017	0.092
J55	Vapour	1.725	80	0.827	[28]	4	0.19	0.19	0.017	0.092
J55	Vapour	1.725	100	0.949	[28]	4	0.19	0.19	0.017	0.092
J55	Vapour	1.725	120	0.894	[28]	4	0.19	0.19	0.017	0.092
J55	Vapour	1.725	140	0.275	[28]	4	0.19	0.19	0.017	0.092
J55	Vapour	1.725	160	0.64	[28]	4	0.19	0.19	0.017	0.092
J55	Vapour	1.725	180	0.351	[28]	4	0.19	0.19	0.017	0.092
J55	Vapour	1.725	200	0.636	[28]	4	0.19	0.19	0.017	0.092

J55	Supercritical	10.34	90	1.105	[28]	4	0.19	0.19	0.017	0.092
N80	Vapour	6.89	90	1.752	[28]	4	0.24	0.036	0.028	0.021
N80	Vapour	1.725	80	0.681	[28]	4	0.24	0.036	0.028	0.021
N80	Vapour	1.725	100	1.053	[28]	4	0.24	0.036	0.028	0.021
N80	Vapour	1.725	120	0.814	[28]	4	0.24	0.036	0.028	0.021
N80	Vapour	1.725	140	0.272	[28]	4	0.24	0.036	0.028	0.021
N80	Vapour	1.725	160	0.191	[28]	4	0.24	0.036	0.028	0.021
N80	Vapour	1.725	200	0.322	[28]	4	0.24	0.036	0.028	0.021
N80	Vapour	1.725	180	0.204	[28]	4	0.24	0.036	0.028	0.021
N80	Supercritical	10.34	90	0.922	[28]	4	0.24	0.036	0.028	0.021
P110	Vapour	6.89	90	2.403	[28]	4	0.26	0.15	0.012	0.01
P110	Vapour	1.725	80	0.948	[28]	4	0.26	0.15	0.012	0.01
P110	Vapour	1.725	100	1.609	[28]	4	0.26	0.15	0.012	0.01
P110	Vapour	1.725	120	0.862	[28]	4	0.26	0.15	0.012	0.01
P110	Vapour	1.725	140	0.41	[28]	4	0.26	0.15	0.012	0.01
P110	Vapour	1.725	160	0.353	[28]	4	0.26	0.15	0.012	0.01
P110	Vapour	1.725	180	0.422	[28]	4	0.26	0.15	0.012	0.01
P110	Vapour	1.725	200	0.95	[28]	4	0.26	0.15	0.012	0.01
P110	Supercritical	10.34	90	0.922	[28]	4	0.26	0.15	0.012	0.01
J55	Vapour	5	20	0.7	[29]	3	0.19	0.049	0.026	0.007
J55	Vapour	5	40	6	[29]	3	0.19	0.049	0.026	0.007
J55	Vapour	5	60	8	[29]	3	0.19	0.049	0.026	0.007
J55	Vapour	5	80	3.9	[29]	3	0.19	0.049	0.026	0.007
J55	Vapour	5	100	0.85	[29]	3	0.19	0.049	0.026	0.007
J55	Vapour	2	80	0.1	[29]	3	0.19	0.049	0.026	0.007
J55	Supercritical	8	80	5.2	[29]	3	0.19	0.049	0.026	0.007
J55	Supercritical	10	80	7.2	[29]	3	0.19	0.049	0.026	0.007
J55	Supercritical	12	80	6.2	[29]	3	0.19	0.049	0.026	0.007
N80	Vapour	5	20	0.7	[29]	3	0.24	0.22	0.028	0.018
N80	Vapour	5	40	5	[29]	3	0.24	0.22	0.028	0.018
N80	Vapour	5	60	9	[29]	3	0.24	0.22	0.028	0.018
N80	Vapour	5	80	3.1	[29]	3	0.24	0.22	0.028	0.018
N80	Vapour	5	100	2	[29]	3	0.24	0.22	0.028	0.018
N80	Vapour	2	80	0.1	[29]	3	0.24	0.22	0.028	0.018
N80	Supercritical	8	80	5.2	[29]	3	0.24	0.22	0.028	0.018
N80	Supercritical	10	80	7.2	[29]	3	0.24	0.22	0.028	0.018
N80	Supercritical	12	80	6.2	[29]	3	0.24	0.22	0.028	0.018
P110	Vapour	5	20	0.8	[29]	3	0.265	0.958	0.042	0.35
P110	Vapour	5	40	5	[29]	3	0.265	0.958	0.042	0.35
P110	Vapour	5	60	10	[29]	3	0.265	0.958	0.042	0.35
P110	Vapour	5	80	4.5	[29]	3	0.265	0.958	0.042	0.35
P110	Vapour	5	100	1.3	[29]	3	0.265	0.958	0.042	0.35
P110	Vapour	2	80	0.2	[29]	3	0.265	0.958	0.042	0.35

P110	Vapour	8	80	5.7	[29]	3	0.265	0.958	0.042	0.35
P110	Vapour	10	80	7.75	[29]	3	0.265	0.958	0.042	0.35
P110	Vapour	12	80	6.4	[29]	3	0.265	0.958	0.042	0.35
P110	Supercritical	8	80	5.7	[29]	3	0.265	0.958	0.042	0.35
P110	Supercritical	10	80	7.75	[29]	3	0.265	0.958	0.042	0.35
P110	Supercritical	12	80	6.4	[29]	3	0.265	0.958	0.042	0.35
K55	Vapour	1	170	0.29	[31]	7				
N80	Vapour	0.4	90	1.689	[32]	3	0.24	0.036	0.028	0.021
N80	Vapour	0.4	90	0.172	[32]	3	0.24	0.036	0.028	0.021
N80	Vapour	0.4	90	0.789	[32]	3	0.24	0.036	0.028	0.021
N80	Vapour	0.4	90	0.621	[32]	3	0.24	0.036	0.028	0.021
N80	Vapour	0.4	90	0.511	[32]	3	0.24	0.036	0.028	0.021
N80	Vapour	4	90	0.55	[36]	5	0.42	0.051	0.005	0.18
N80	Vapour	4	90	1.25	[36]	5	0.42	0.051	0.005	0.18
N80	Vapour	4	90	3.55	[36]	5	0.42	0.051	0.005	0.18
N80	Vapour	4	90	4.95	[36]	5	0.42	0.051	0.005	0.18
L80	Vapour	4	65	8.5	[34]	2	0.3	0.85		
L80	Supercritical	8	65	9.9	[34]	2	0.3	0.85		
L80	Supercritical	12	65	11	[34]	2	0.3	0.85		
L80	Vapour	4	90	6.1	[34]	2	0.3	0.85		
L80	Supercritical	8	90	3.4	[34]	2	0.3	0.85		
L80	Supercritical	12	90	4.8	[34]	2	0.3	0.85		
L80	Supercritical	15	50	0.375	[35]	30	0.315	0.04	0.01	0.11
L80	Supercritical	15	50	3.534	[35]	7	0.315	0.04	0.01	0.11
L80	Supercritical	30	50	2.774	[35]	7	0.315	0.04	0.01	0.11
L80	Vapour	0.5	60	1.5568	[36]	30	0.22	1.2	0.5	
L80	Vapour	0.5	90	1.0627	[36]	30	0.22	1.2	0.5	
L80	Vapour	0.5	150	1.3941	[36]	30	0.22	1.2	0.5	
L80	Vapour	0.5	60	1.467	[36]	30	0.22	1.2	0.5	
L80	Vapour	0.5	90	0.7794	[36]	30	0.22	1.2	0.5	
L80	Vapour	0.5	150	2.0835	[36]	30	0.22	1.2	0.5	
L80	Vapour	0.5	60	1.1466	[36]	30	0.22	1.2	0.5	
L80	Vapour	0.5	90	0.9401	[36]	30	0.22	1.2	0.5	
L80	Vapour	0.5	150	0.9807	[36]	30	0.22	1.2	0.5	
L80	Vapour	0.5	60	1.0967	[36]	30	0.22	1.2	0.5	
L80	Vapour	0.5	90	0.6833	[36]	30	0.22	1.2	0.5	
L80	Vapour	0.5	150	1.0032	[36]	30	0.22	1.2	0.5	
L80	Vapour	0.1	20	0.56	[37]	3	0.17	0.81	0.014	0.003
L80	Vapour	0.1	20	0.49	[37]	3	0.21	0.82	0.015	0.031
L80	Vapour	0.1	20	0.45	[37]	3	0.17	0.81	0.014	0.003
L80	Vapour	0.1	20	0.52	[37]	3	0.21	0.82	0.015	0.031
L80	Vapour	0.1	20	0.89	[37]	3	0.17	0.81	0.014	0.003
L80	Vapour	0.1	20	0.29	[37]	3	0.21	0.82	0.015	0.031

L80	Vapour	0.3	20	1.29	[37]	3	0.17	0.81	0.014	0.003
L80	Vapour	0.3	20	0.71	[37]	3	0.21	0.82	0.015	0.031
L80	Vapour	0.3	20	1.26	[37]	3	0.17	0.81	0.014	0.003
L80	Vapour	0.3	20	0.8	[37]	3	0.21	0.82	0.015	0.031
L80	Vapour	0.3	20	1.13	[37]	3	0.17	0.81	0.014	0.003
L80	Vapour	0.3	20	0.82	[37]	3	0.21	0.82	0.015	0.031
T95	Supercritical	41.37	38	15	[38]	7	0.33	1.01	0.03	0.79
T95	Supercritical	41.37	38	20	[38]	7	0.33	1.01	0.03	0.79
T95	Supercritical	41.37	38	17	[38]	7	0.33	1.01	0.03	0.79
T95	Supercritical	41.37	38	17.5	[38]	7	0.33	1.01	0.03	0.79
Q125	Supercritical	41.37	38	3.2	[38]	7	0.26	0.91	0.04	0.26
Q125	Supercritical	41.37	38	9.5	[38]	7	0.26	0.91	0.04	0.26
Q125	Supercritical	41.37	38	10	[38]	7	0.26	0.91	0.04	0.26
Q125	Supercritical	41.37	38	10	[38]	7	0.26	0.91	0.04	0.26
C110	Supercritical	41.37	38	13	[38]	7	0.3	1.01	0.01	0.78
C110	Supercritical	41.37	38	14.5	[38]	7	0.3	1.01	0.01	0.78
C110	Supercritical	41.37	38	9	[38]	7	0.3	1.01	0.01	0.78
P110	Vapour	4	100	6.1843	[39]	5	0.19		0.028	0.028
P110	Vapour	4	160	0.8754	[39]	5	0.19		0.028	0.028
P110	Vapour	4	90	0.9394	[40]	3				
P110	Vapour	4	110	0.4491	[40]	3				
P110	Vapour	0.1	100	0.64	[41]	7	0.26		0.028	0.028
P110	Vapour	2	100	0.76	[41]	7	0.26		0.028	0.028
P110	Vapour	4	100	0.91	[41]	7	0.26		0.028	0.028
P110	Vapour	6	100	0.83	[41]	7	0.26		0.028	0.028
Q125	Vapour	1	30	1.012	[42]	7	0.2	1.03	0.2	0.3
Q125	Vapour	2	30	0.9	[43]	7	0.15	0.46	0.2	0.15
Q125	Vapour	2	60	2.8	[43]	7	0.15	0.46	0.2	0.15
Q125	Vapour	2	90	3.6	[43]	7	0.15	0.46	0.2	0.15
Q125	Vapour	2	120	2.4	[43]	7	0.15	0.46	0.2	0.15
20Cr-25Ni	Supercritical	9.5	50	0.0003	[44]	4	0.02	20	25	4.5
20Cr-25Ni	Supercritical	13	80	0.001	[44]	4	0.02	20	25	4.5
20Cr-25Ni	Supercritical	16	110	0.0001	[44]	4	0.02	20	25	4.5
20Cr-25Ni	Supercritical	18.2	130	0.00005	[44]	4	0.02	20	25	4.5
20Cr-25Ni	Supercritical	9.5	50	0.00006	[44]	4	0.02	20	25	4.5
20Cr-25Ni	Supercritical	13.5	80	0.00009	[44]	4	0.02	20	25	4.5
20Cr-25Ni	Supercritical	17	110	0.00011	[44]	4	0.02	20	25	4.5
20Cr-25Ni	Supercritical	21.5	130	0.00005	[44]	4	0.02	20	25	4.5
13Cr	Supercritical	9.5	50	0.003	[44]	4	0.195	13		

13Cr	Supercritical	13	80	0.0038	[44]	4	0.195	13	
13Cr	Supercritical	16	110	0.009	[44]	4	0.195	13	
13Cr	Supercritical	18.2	130	0.003	[44]	4	0.195	13	
13Cr	Supercritical	9.5	50	0.00033	[44]	4	0.195	13	
13Cr	Supercritical	13.5	80	0.0006	[44]	4	0.195	13	
13Cr	Supercritical	17	110	0.0008	[44]	4	0.195	13	
13Cr	Supercritical	21.5	130	0.0004	[44]	4	0.195	13	
22Cr	Supercritical	9.5	50	0.0007	[44]	4	0.03	22	5	3
22Cr	Supercritical	13	80	0.0008	[44]	4	0.03	22	5	3
22Cr	Supercritical	16	110	0.0004	[44]	4	0.03	22	5	3
22Cr	Supercritical	18.2	130	0.0001	[44]	4	0.03	22	5	3
22Cr	Supercritical	9.5	50	0.00006	[44]	4	0.03	22	5	3
22Cr	Supercritical	13.5	80	0.0001	[44]	4	0.03	22	5	3
22Cr	Supercritical	17	110	0.00014	[44]	4	0.03	22	5	3
22Cr	Supercritical	21.5	130	0.00006	[44]	4	0.03	22	5	3
13Cr	Vapour	0.1	60	0.002	[45]	29.167	0.46	13.39	0.13	0.03
13Cr	Vapour	6	60	0.0002	[45]	29.167	0.46	13.39	0.13	0.03
1Cr	Vapour	0.1	60	0.0059	[45]	29.167	0.43	1.05	0.04	0.22
1Cr	Vapour	6	60	0.0015	[45]	29.167	0.43	1.05	0.04	0.22
13Cr	Vapour	0.2	50	0.1	[46]	90	0.029	12.78	5.12	2.23
22Cr	Vapour	0.2	50	0.01	[46]	90	0.23	22.91	5.65	3.21
P110	Vapour	0.2	50	0.18	[46]	90	0.25	1.06	0.025	0.65
J55	Supercritical	9.5	70	0.1	[47]	12.5			
J55	Supercritical	9.5	70	0.1	[47]	12.5			
N80	Supercritical	9.5	70	0.1	[47]	12.5			
N80	Supercritical	9.5	70	0.1	[47]	12.5			
J55	Supercritical	9.5	70	2	[47]	4.67			
J55	Supercritical	9.5	70	0.2	[47]	4.67			
N80	Supercritical	9.5	70	1.15	[47]	4.67			
N80	Supercritical	9.5	70	0.2	[47]	4.67			
J55	Vapour	0.5	65	3.3	[48]	2	0.36	0.051	0.009
J55	Vapour	1	65	6.7	[48]	2	0.36	0.051	0.009
J55	Vapour	1.5	65	5.9	[48]	2	0.36	0.051	0.009
J55	Vapour	2.5	65	4.7	[48]	2	0.36	0.051	0.009
J55	Vapour	3	65	3.5	[48]	2	0.36	0.051	0.009
J55	Vapour	5	65	3.95	[48]	2	0.36	0.051	0.009
J55	Vapour	7	65	5.2	[48]	2	0.36	0.051	0.009
J55	Supercritical	9	65	5.2	[48]	2	0.36	0.051	0.009
J55	Supercritical	11	65	5.2	[48]	2	0.36	0.051	0.009
J55	Supercritical	13	65	5.2	[48]	2	0.36	0.051	0.009
J55	Supercritical	15	65	5.2	[48]	2	0.36	0.051	0.009
J55	Vapour	5	30	0.09	[49]	3	0.38	0.09	
J55	Vapour	5	48	0.088	[49]	3	0.38	0.09	

J55	Vapour	5	55	0.13	[49]	3	0.38	0.09		
J55	Vapour	5	65	0.148	[49]	3	0.38	0.09		
N80	Vapour	0.5	50	6.5	[50]	2	0.33	0.013	0.026	0.016
N80	Vapour	1	50	9.5	[50]	2	0.33	0.013	0.026	0.016
N80	Vapour	2	50	12	[50]	2	0.33	0.013	0.026	0.016
N80	Vapour	3	50	9.5	[50]	2	0.33	0.013	0.026	0.016
N80	Vapour	4	50	9	[50]	2	0.33	0.013	0.026	0.016
N80	Vapour	5	50	3.8	[50]	2	0.33	0.013	0.026	0.016
N80	Supercritical	10	50	1.8	[50]	2	0.33	0.013	0.026	0.016
N80	Supercritical	10	65	8.4	[50]	2	0.33	0.013	0.026	0.016
N80	Supercritical	10	80	11.8	[50]	2	0.33	0.013	0.026	0.016
N80	Vapour	0.15	100	0.75	[51]	3	0.26	0.148	0.028	0.028
N80	Vapour	0.6	100	1.15	[51]	3	0.26	0.148	0.028	0.028
N80	Vapour	1	100	2.25	[51]	3	0.26	0.148	0.028	0.028
N80	Vapour	4	100	7.2	[51]	3	0.26	0.148	0.028	0.028
N80	Vapour	0.1	80	4.65	[52]	3	0.19	0.55		0.14
3Cr	Vapour	0.1	80	2.9	[52]	3	0.1	3.75		0.25
3Cr	Vapour	0.1	80	3.25	[52]	3	0.11	3.3		0.21
N80	Vapour	8	45	0.056	[53]	32	0.29	0.24	0.08	0.09
L80	Vapour	1	25	0.2334	[54]	2	0.22	0.013		
L80	Vapour	4	25	0.3905	[54]	2	0.22	0.013		
L80	Vapour	6	25	0.4044	[54]	2	0.22	0.013		
L80	Vapour	1	25	0.254	[54]	2	0.22	0.013		
L80	Vapour	4	25	0.347	[54]	2	0.22	0.013		
L80	Vapour	6	25	0.4681	[54]	2	0.22	0.013		
L80	Vapour	0.1	80	0.13	[55]	5	0.43		0.25	
L80	Vapour	0.1	80	0.13	[55]	5	0.43	0.95	0.25	
L80	Vapour	0.1	80	0.3	[55]	5	0.11	3.4	0.15	0.6
C110	Supercritical	10.8	120	0.55	[56]	7	0.27		0.04	0.72
P110	Vapour	5	90	1.12	[57]	15	0.25	0.15	0.032	0.27
P110	Vapour	5	90	1.08	[57]	15	0.26	2.99	0.043	0.19
P110	Vapour	5	90	1.57	[57]	15	0.25	5.11	0.041	0.21
P110	Vapour	0.5	120	0.03	[58]	1	0.26			0.01
P110	Vapour	1.5	120	2.23	[58]	1	0.26			0.01
P110	Vapour	3	120	1.1	[58]	1	0.26			0.01
N80	Vapour	0.5	120	0.03	[58]	1	0.24			0.021
N80	Vapour	1.5	120	1.5	[58]	1	0.24			0.021
P110	Vapour	0.1	90	4.2	[59]	5	0.22	0.18	0.01	0.03